Theor Chem Acc (2007) 117:417–429
DOI 10.1007/s00214-006-0169-2

REGULAR ARTICLE

Atomic radical—molecule reactions F + $CH_3C{\equiv}CH$: mechanistic study

Ji-Lai Li · Cai-Yun Geng · Xu-Ri Huang · Chia-Chung Sun

Received: 21 May 2006 / Accepted: 10 August 2006 / Published online: 19 September 2006

Abstract The reaction of atomic radical F with propyne has been studied theoretically using ab initio quantum chemistry methods and transition state theory. The potential energy surface was calculated at the CCSD(T)/aug-cc-pVDZ (single-point) level using the UMP2/6-311++G(d,p) optimized structures. Two reaction mechanisms including the addition–isomerization–elimination reaction mechanism and the directed hydrogen abstraction reaction mechanism are considered. For the hydrogen abstraction reactions, i.e., the most probable evolution pathway in the title reaction, the HF formation occurs via direct abstraction mechanism dominantly and the H atom picked up by the atomic radical F should come mostly from the methyl group of normal propyne. On the other hand, for the addition–isomerization–elimination mechanism, the most feasible pathway should be the atomic radical F attacking on the C≡C triple bond in propyne ($CH_3C{\equiv}CH$) to form a weakly-bound adduct A1 with no barrier, followed by F addition to the C≡C triple bond to form the low-lying intermediate isomer 5. Subsequently, isomer 5 directly dissociates to P3 H_2CCCHF + H via transition state $TS_{5/P3}$. The other reaction pathways on the doublet PES are less competitive due to thermodynamical or kinetic factors. Furthermore, based on the analysis of the kinetics of all channels through which the addition and abstraction reaction proceed, we expect that the competitive power of reaction channels may vary with experimental conditions for the title reaction. The present work will provide useful information for understanding the processes of atomic radical F reaction with other unsaturated hydrocarbons.

Keywords Reaction mechanism · Potential energy surface (PES) · Atomic radical F · Propyne

1 Introduction

The reactivity of the atomic radical F is an interesting research topic because of the complicated nature of the reaction mechanism involved in these reactions and its importance in many industrial applications. A variety of reaction mechanisms are involved in its reaction with different molecules. The reactions of atomic radical F with unsaturated hydrocarbons have been studied extensively, both theoretically and experimentally [1–19]. It was found that this class of reactions proceed primarily by the addition of atomic radical F to the double/triple bond of the hydrocarbon molecules to form long-lived chemical activated radical complexes, which further decompose unimolecularly to give predominantly hydrogen atoms or methyl radicals. In contrast, in the atomic radical F reaction with methane [20–23], the reaction mainly occurs through an abstraction mechanism to produce a HF molecule and a methyl radical (CH_3) in which the CH_3 part is largely a spectator during the reaction process. Recently, Lee and coworkers [7] carried out the universal crossed beam study on the reaction dynamics of atomic radical F reaction with the propyne molecule with both single and triple bonds, in which reactions occur through both direct abstraction and complex formation mechanisms. As

This material is available from author via E-mail.

J.-L. Li · C.-Y. Geng · X.-R. Huang (✉) · C.-C. Sun
State Key Laboratory of Theoretical and Computational Chemistry, Institute of Theoretical Chemistry, Jilin University, Changchun 130023, People's Republic of China
e-mail: lijilai2008@yahoo.com

shown in Eqs. (1)–(2), two different reaction channels of the F + CH_3CCH reaction have been clearly identified: (1) the substitution of F for H occurs mainly via a complex formation mechanism, producing reaction products with some contribution from a direct reaction mechanism; (2) the HF product, however, appears to be dominantly forward scattered relative to the F atom beam direction, suggesting that the HF formation occurs via a direct abstraction mechanism. The H formation channel is found to be the major reaction pathway, while the HF formation channel is also significant [7].

$$F + CH_3CCH \rightarrow C_3H_3F + H \quad (81\%) \tag{1}$$

$$F + CH_3CCH \rightarrow C_3H_3 + HF \quad (19\%) \tag{2}$$

However, in an investigation [6] of the mechanism for the reaction of atomic radical F with propene, three different reaction channels of the F + $C_2H_3CH_3$ reaction have been identified [as shown in Eqs. (3)–(5)]: (1) the H atom formation channel takes place through some direct reaction mechanism as well as likely to be a long-lived complex formation process; (2) the CH_3 formation process mainly proceeds through a long-lived complex formation mechanism and (3) HF formation shows clearly that a direct pickup type reaction mechanism is responsible for this channel. Experimental results show that the CH_3 formation is the most important reaction pathway for the title reaction, while both H and HF formation channels are also significant.

$$F + C_2H_3CH_3 \rightarrow C_3H_5F + H \quad (15\%) \tag{3}$$

$$F + C_2H_3CH_3 \rightarrow C_2H_3F + CH_3 \quad (65\%) \tag{4}$$

$$F + C_2H_3CH_3 \rightarrow C_3H_5 + HF \quad (19\%) \tag{5}$$

For the discrepancies, a computational study is very desirable to gain insight into the title reaction mechanism. To our knowledge, the nature of different reaction channels in the atomic radical F reactions with hydrocarbon molecules has not been investigated in detail in all previous experiments and no report is found about the theoretical study on the title reaction. In addition, recently, the doublet potential energy surfaces (DPESs) of the analogous F + propene reaction have been built up by us [18]. In the F + propene reaction, we have shown that simple hydrogen abstraction reactions and F addition reactions involve many more prereactive complexes than had previously been thought. Now, the sequential question is whether the mechanism of the title reaction F + propyne is similar to the F + propene reaction or not?

In view of the potential importance and the rather limited information, the detailed theoretical study on the doublet potential energy surfaces (DPESs) of the title reactions is therefore very desirable. The main objectives of the present article are to (1) provide the elaborated isomerization and dissociation channels on the C_3H_4F DPESs; (2) investigate the site specific effect of the title reaction to give deep insight into the mechanism of F + hydrocarbons reaction; (3) make comparisons on the mechanisms between halogen (F) with propene and propyne. From this present, one can gain deep insight into the mechanism of F + propene reaction as the elaborated isomerization and dissociation channels on the C_3H_6F DPESs were provided rationally and the site specific effects were pointed out unambiguously. Some conclusions that are made in this article may be helpful to resolve the question mentioned above and for further theoretical and experimental studies of this reaction.

However, theoretical studies on the reactions involving radical addition to alkenes showed that such reactions are difficult to describe theoretically and that the calculated energies are sensitive to theoretical levels [24]. In a theoretical study of the reaction between a chlorine atom and ethylene, Braña [25] compared the potential energy surfaces computed at different theoretical levels and concluded that extreme care should be taken to choose an appropriate theoretical level for calculations involving radicals. Additionally, Zhang [16] proposed that for systems similar to the title reaction, the geometrical parameters for weakly bound structures and transition structures are more sensitive to theoretical level than other equilibrium structures. To obtain reliable geometrical parameters, the MP2/6-31G(d,p) level of theory or higher is needed [16]. Furthermore, rational conclusions of the reaction mechanisms of F + propene were draw at the CCSD(T)cc-pVTZ//UMP2/6-311++G(d,p) + ZPE levels of theory [18]. Therefore, the title reaction mechanisms were investigated and a detailed ground state doublet potential energy surface was plotted at the CCSD(T)/aug-cc-pVDZ//UMP2/6-311++G(d,p) + ZPE levels of theory. As the conclusions reached are supported by the reported experimental results, we consider that the theoretical methods employed are appropriate and the results (geometries and single-point energies) are acceptable.

2 Computational method details

All the calculations were carried out on the SGI O3800 Servers using the GAUSSIAN98 program package [26]. All geometries of the reactants, complexes, products, intermediates and transition states (TS) have been optimized with the unrestricted Møller–Plesset second-order perturbation UMP2(FULL) [27] method using the 6-311G, 6-311G(d,p) and 6-311++G(d,p) basis set respectively. The presence of diffuse functions in the

basis set allows for an appropriate representation of the dispersion forces that should play an important role in the stabilization of the weakly bound structures considered in this work [25,28]. Vibrational frequencies, also calculated at the same level of theory, have been used to characterize stationary points, zero-point energy (ZPE) corrections calculations. The number of imaginary frequencies for intermediates and transition states are 0 and 1, respectively. The ZPE and vibrational frequencies were scaled by a factor of 0.95 for anharmonicity correction [29]. To confirm that the transition states connect between designated intermediates, intrinsic reaction coordinate (IRC) [30] calculations were performed at the UMP2(FULL)/6-311++G(d,p) level of theory.

For the purpose of obtaining more reliable energies of various structures, the coupled–cluster CCSD(T) method with single, double and perturbative treatment of triple excitations [31] in conjunction with Dunning's correlation-consistent augmented basis sets aug-cc-pVDZ[32,33] was used. The UMP2(FULL)/6-311++G(d,p) optimized geometries were used for the single-point coupled cluster calculations without reoptimization at the CCSD(T)/aug-cc-pVDZ levels.

The major problem in the application of unrestricted single determinant reference wave function is that of contamination with higher spin states. The severe spin contamination could lead to a deteriorated estimation of the barrier height [34,35]. We have examined the spin contamination before and after annihilation for the radical species and transition states involved in the F + CH_3CCH reaction. For doublet systems, the expectation values of $\langle S^2 \rangle$ after annihilation range from 0.80 to 0.75 (the exact value for a pure doublet is 0.75). This suggests that the wave function is not severely contaminated by states of higher multiplicity [36,37].

Recent studies on systems similar to the ones considered in this article concluded that the use of spin annihilation techniques to generate spin-projected energies is mandatory for calculations of both reaction energies and barrier heights [24]. All UMP2 energy values reported in this work correspond to spin-projected calculations using Schlegel's algorithm [38]. On the other hand, Stanton [39] has shown that all spin contamination is essentially removed from the coupled cluster wave functions. Considering even with modest spin contamination, the position and height of the barriers may be affected [40], several points along the reaction path (IRC) were optimized at the UMP2 level, followed by single point calculations at the CCSD(T) level to verify the negative barriers at the reactant entrance, since the reaction path should be less sensitive to spin contamination [41]. Therefore, we expect that the CCSD(T) calculations reported in this work are, in this regard, reliable.

The thermodynamic functions ($\Delta \boldsymbol{H}$, $\Delta \boldsymbol{S}$, and $\Delta \boldsymbol{G}$) were estimated within the ideal gas, rigid-rotor, and harmonic oscillator approximations. A temperature of 298.15 K and a pressure of 1 atm. were assumed.

3 Results and discussion

For the present C_3H_4F system, 1 adduct, 2 intermediate complexes (loose structure), 9 intermediate isomers, 19 transition states and 5 products are obtained at the UMP2(FULL)/6-311G, UMP2(FULL)/6-311G(d,p) and UMP2(FULL)/6-311++G(d,p) levels of theory, respectively. The structures of the reactants, adduct, intermediate complexes and isomers, transition states and products are depicted in Fig. 1. The symbol $\mathbf{TS}_{x/y}$ is used to denote a transition state, where x and y are the corresponding isomers or products. By means of the interrelation among the reactants, complexes, isomers, transition states and products as well as the corresponding relative energies, the schematic profiles of the potential energy surface are depicted as shown in Fig. 2, where the values are the CCSD(T)/UMP2 + ZPE relative energies. The schematic map of reaction mechanisms and activation energies (E) of the title reaction is shown in Scheme 1. The calculated energetic data ($\Delta \boldsymbol{E}$, $\Delta \boldsymbol{H}$, $\Delta \boldsymbol{S}$ and $\Delta \boldsymbol{G}$) of various complexes, isomers, transition states and products are listed in Table 1. It should be noted that the energy of F + propyne is set at zero as a reference for other species for convenient discussion. It should be stressed at this point that some apparent inconsistencies appearing in Fig. 2 and in Table 1 in this work arise from the use of single-point spin-projected energies [38] (see, e.g., in Fig. 2, where $TS_{C1/P1}$ lies 2.60 kcal/mol below C1, etc.). We checked that all the unprojected energy profiles are topologically consistent. Bearing in mind the limitation (the use of harmonic frequencies for the highly anharmonic intramolecular vibrations) inherent in our calculations, this may not be accurate enough for the rather flexible transition states and the complexes. When all comes to all, however, the results are acceptable.

3.1 Analysis of reaction mechanism of atomic radical F with propyne

As the atomic radical F • ("•" denotes the unpaired single electron) can have either abstraction or addition mechanism, two distinguishable type initial attacks have

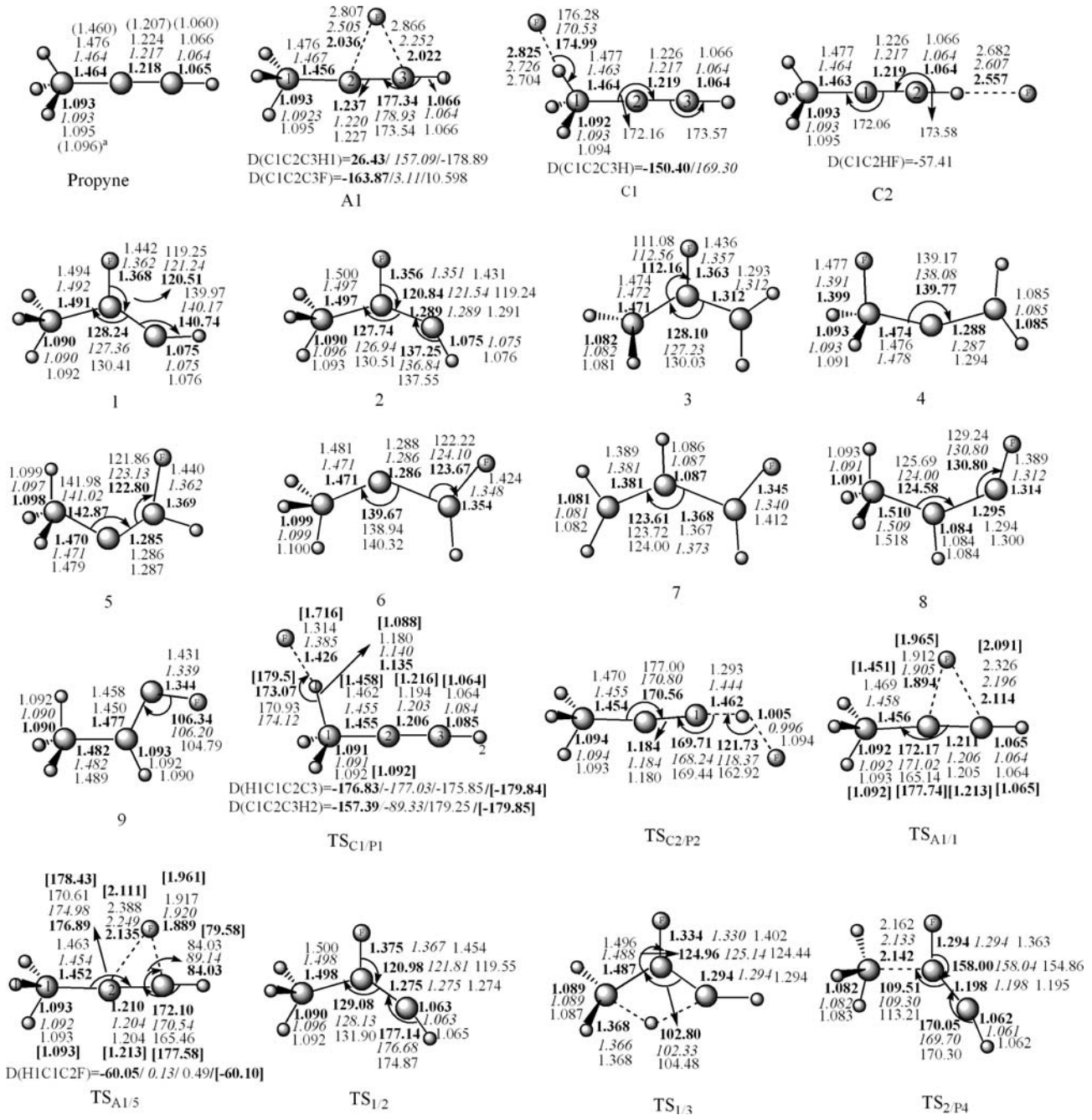

Fig. 1 Optimized geometries of the reactants, adduct, weakly-bound complexes, doublet intermediate isomers, transition states and products for the F + Propyne reaction. Bond distances are in angstroms and angles are in degrees. Numbers in *bold, italics, normal* and *square brackets* show the structures at the UMP2/6-311++G(d,p), UMP2/6-311G(d,p), UMP2/6-311G and Max{CCSD(T)/aug-cc-pVDZ}//IRC{UMP2/6-311++G(d,p)} + ZPE levels of theory, respectively. Numbers in *parenthesis* are the experimental values. *a* ref [42], *b* ref [43], *c* ref [44], *d* ref [45]

been revealed for the radical–molecule reaction F + propyne, namely, the attack on hydrogen (direct and/or two-steps hydrogen abstraction) and the addition to the C≡C triple bond (addition–isomerization–elimination). A detailed discussion on the title reaction mechanisms as shown in Fig. 2 is given as follows.

3.1.1 Addition–isomerization–elimination reaction mechanism

Firstly, the atomic radical F (^{2}F) and propyne ($CH_3C{\equiv}CH$) approach each other forming a weakly-bound adduct 1 (A1). Adduct A1 contains two C···F bonds (see

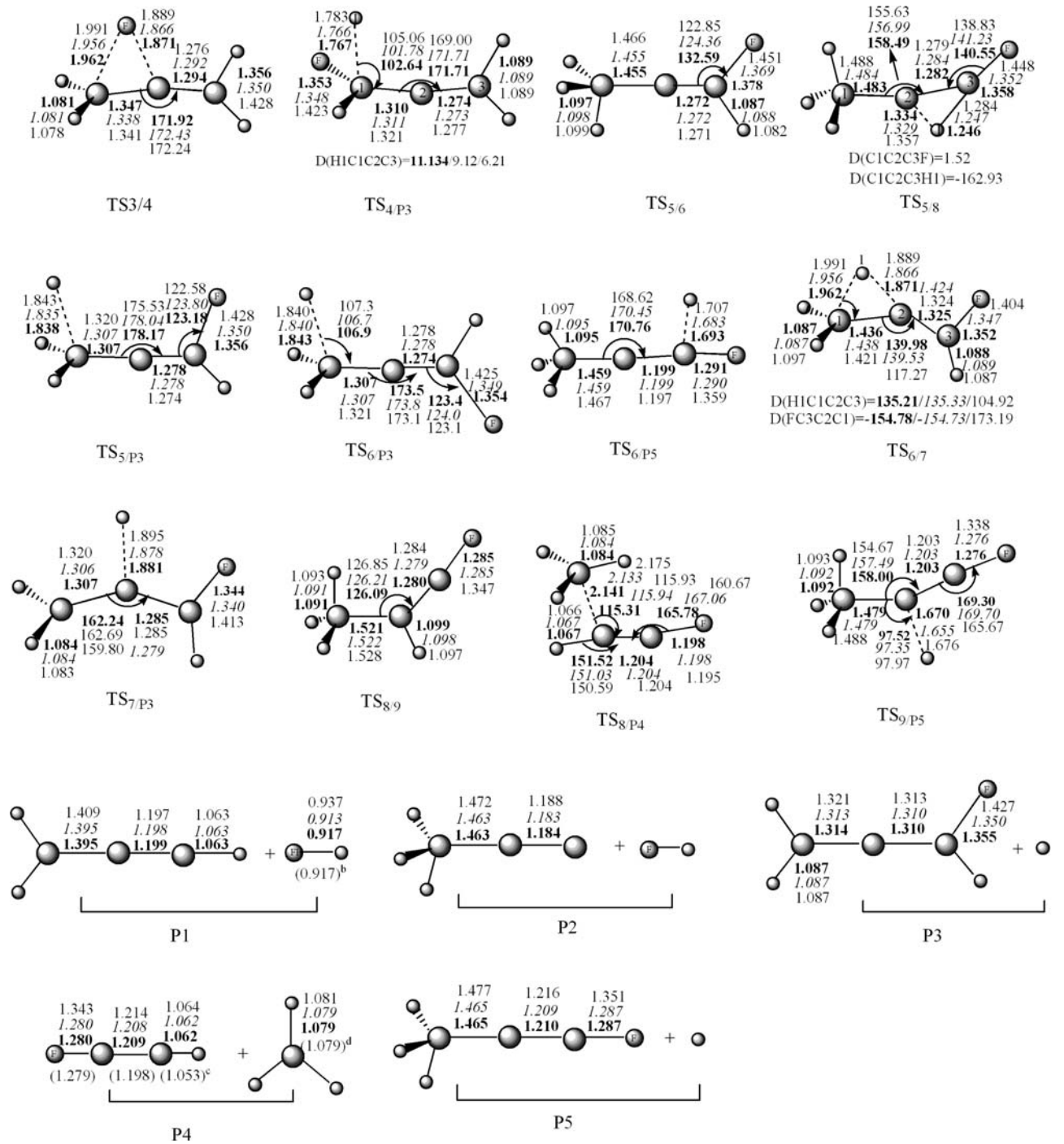

Fig. 1 continued

Fig. 1), which stabilize A1 by 7.77 kcal/mol relative to the reactant R F + $CH_3C{\equiv}CH$ (0.0 kcal/mol). It is obvious that this addition process is a barrier-free association [16, 18]. Then, adduct A1 can undergo two concerted three-center F-shifts, one of the F-shift is the C3···F bond elongated and the C2···F bond shortened ($TS_{A1/1}$) leading to another low-lying intermediate isomer 1 CH_3CFCH (1, −43.96) with large exothermicity, while the other is the C3···F bond shortened and the C2···F bond elongated ($TS_{A1/5}$) to produce the low-lying intermediate isomer 5 CH_3CCHF (5, −40.28) with larger exothermicity. The A1→1 and A1→5 energy barriers are 0.4 and 0.16 kcal/mol, respectively, at Max{CCSD(T)/aug-cc-pVDZ}//IRC{UMP2/6-311++G(d,p)} + ZPE level of

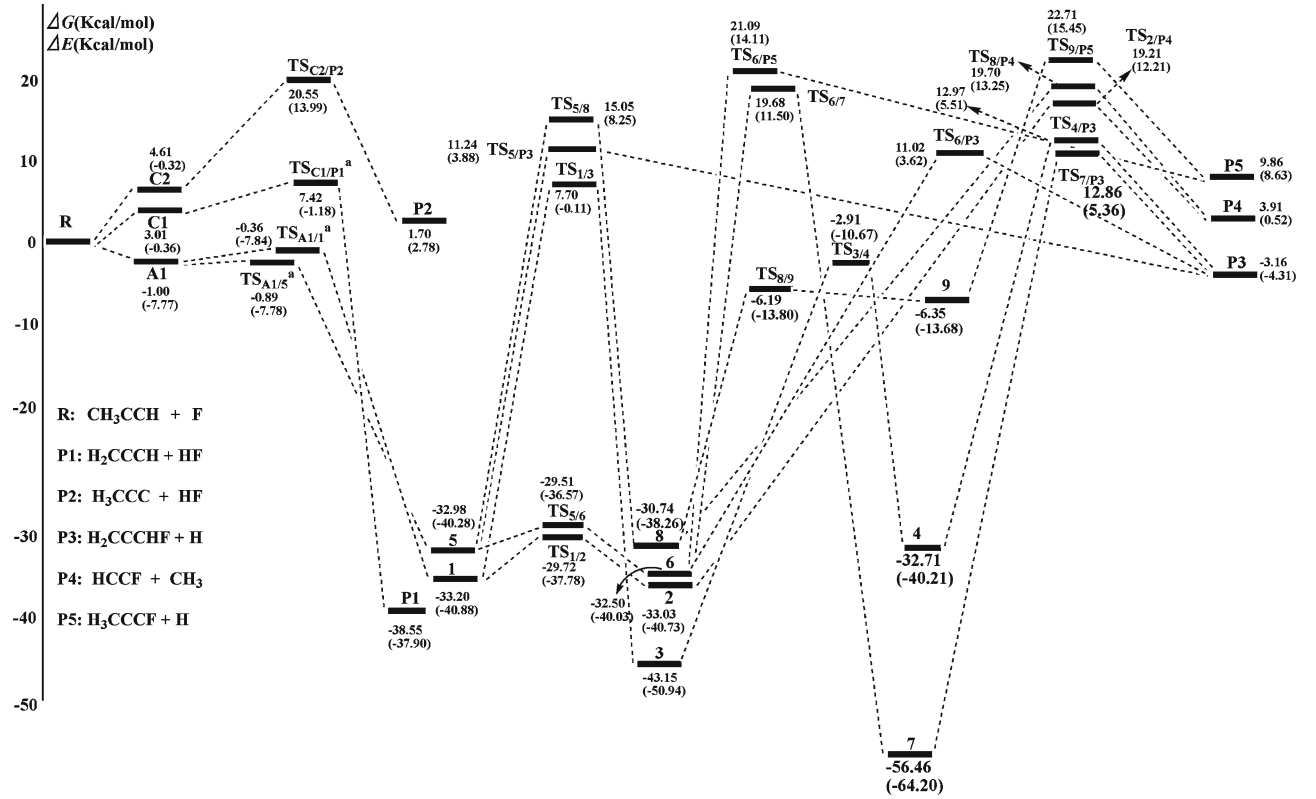

Fig. 2 The potential energy surfaces (PESs) for the F + propyne reaction. The values in parentheses and nude are relative energies and Gibbs free energies obtained at the CCSD(T)/aug-cc-pVDZ//UMP2/6-311++G(d,p)+ZPE level of theory *a* At the Max{CCSD(T)/aug-cc-pVDZ}//IRC{UMP2/6-311++G(d,p)} + ZPE level of theory

theory. To our knowledge, it is the first time that the existence of a prereaction complex in the title reactions has been reported and the addition features of PES we predicted are very similar with that of F + ethylene [16] and F + propene [18].

The overall process R→A1→1 and R→A1→5 are both associated with the addition of the atomic radical F to the C≡C triple bond of $CH_3C{\equiv}CH$. Such processes, characteristic of radical association reactions and typical F-addition mechanism [18], gives rise to loose transition states. As shown in Fig. 1, structural features of the insertion transition states $TS_{A1/1}$ and $TS_{A1/5}$ are more similar to the adduct A1 than to the isomer **1** and **5** respectively. This is consistent with the Hammond postulate which states that a transition state will be structurally and energetically similar to the species (reactant, intermediate or product) nearest to it on the reaction path. In analogous theoretical investigations, F + $CH_2 = CH_2$ [16] and F + $CH_3CH = CH_2$ [18], the same conclusion was also made. With the large heat released from the addition processes, the intermediate isomers 1 and 5 can easily undergo eight isomerization and dissociation pathways that can be expressed as follows:

Path1 RP3 R → A1 → $TS_{A1/5}$ → 5 → $TS_{5/P3}$ → P3
Path2 RP3 R → A1 → $TS_{A1/5}$ → 5 → $TS_{5/6}$ → 6 → $TS_{6/P3}$ → P3
Path3 RP3 R → A1 → $TS_{A1/5}$ → 5 → $TS_{5/6}$ → 6 → $TS_{6/7}$ → 7 → $TS_{7/P3}$ → P3
Path4 RP3 R → A1 → $TS_{A1/1}$ → 1 → $TS_{1/3}$ → 3 → $TS_{3/4}$ → 4 → $TS_{4/P3}$ → P3
Path5 RP4 R → A1 → $TS_{A1/1}$ → 1 → $TS_{1/2}$ → 2 → $TS_{2/P4}$ → P4
Path6 RP4 R → A1 → $TS_{A1/5}$ → 5 → $TS_{5/8}$ → 8 → $TS_{8/P4}$ → P4
Path7 RP5 R → A1 → $TS_{A1/5}$ → 5 → $TS_{5/6}$ → 6 → $TS_{6/P5}$ → P5
Path8 RP5 R → A1 → $TS_{A1/5}$ → 5 → $TS_{5/8}$ → 8 → $TS_{8/9}$ → 9 → $TS_{9/P5}$ → P5

In terms of small species in products, the title reaction has three different channels in the addition–isomerization–elimination reaction mechanism, i.e. (I) the CH_2CCHF (fluoroallene) + H formation channels, Path 1–4; (II) the HCCF (fluoroethyne) + CH_3 formation channels, Path 5/6 and (III) the CH_3CCF (fluoropropyne) + H formation channels, Path 7/8.

Scheme 1 Reaction mechanism and activation energies (kcal/mol) of the F + propyne reaction. Activation energies are calculated at the CCSD(T)/aug-cc-pVDZ//UMP2/6-311++G(d,p) + ZPE level of theory

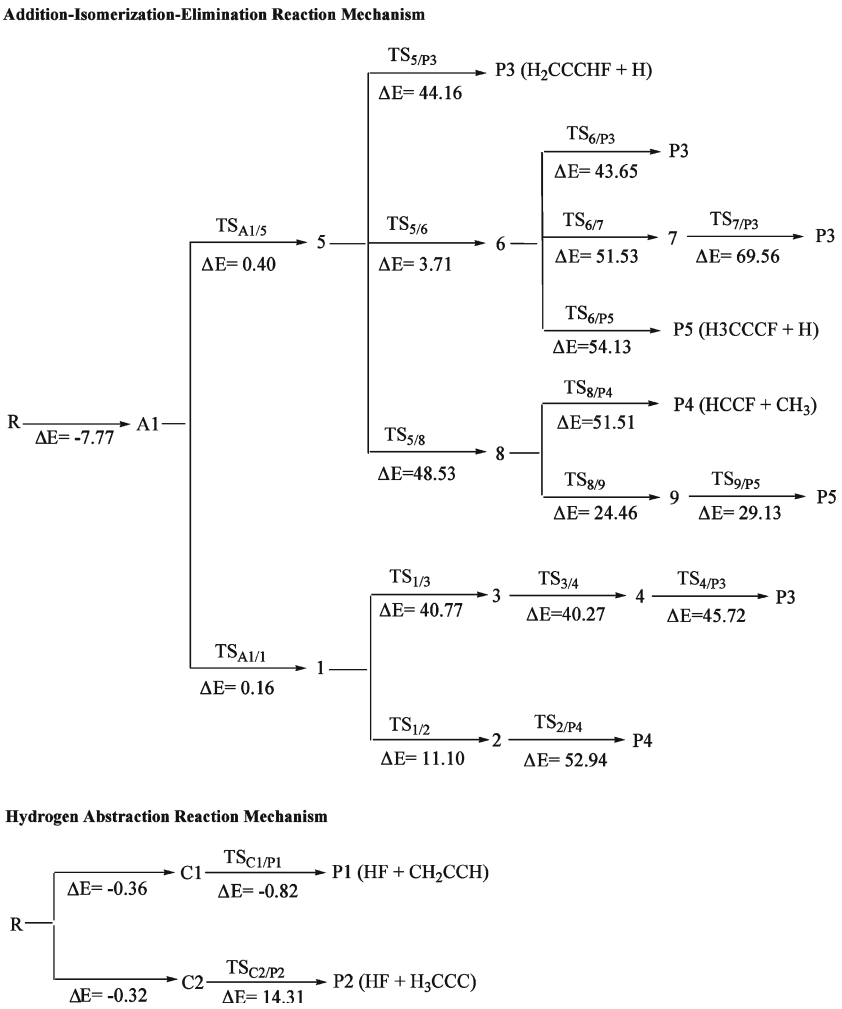

I. The CH_2CCHF (fluoroallene) + H formation channel

Obviously, for the first three pathways of this channel, they possess the same initial steps of the reaction, i.e. R → A1 → $TS_{A1/5}$ → 5. The difference of the three pathways is the way how intermediate isomer 5 changes to P3. Starting from the adduct A1, $CH_3(C\cdots F\cdots C)_{ring}H$ (−7.77), the pathway Path1 RP3 can reach the products P3 CH_2CCHF + H easily by going through transition state $TS_{A1/5}$(−7.78), intermediate isomer 5 CH_3CCHF (−40.28) and $TS_{5/P3}$ (3.88). As shown in Fig. 1, the geometry of transition state $TS_{5/P3}$ calculated at the UMP2/6-311++G(d,p) level is found to have an elongated C···H bond length (r_{C-H} = 1.838 Å). Most importantly, this geometry is indicative of an "late" transition state, corresponding to a C–H distance significantly longer than the equilibrium bond length (1.098 Å in 5). Since the relative energy of the rate-determining transition state $TS_{5/P3}$ lies 3.88 kcal/mol higher than the reactants, the rate of this pathway should be considerably fast. Furthermore, since the pathway Path1 RP3 has no transition state in the first reaction step and tight structure isomers and transition states to the products, it should possess the character of negative temperature dependence in low-temperature ranges. Alternatively, in pathway Path2 RP3, intermediate isomer 5 first transforms to 6 easily via overcoming the transition state $TS_{5/6}$ (−36.57), a 3.71 kcal/mol energy barrier. Then, 6 can eliminate a methyl H-atom, by passing through $TS_{6/P3}$, and dissociate to educts P3. Although the rate-determining transition states $TS_{6/P3}$ in Path2 RP3 is slightly lower than that ($TS_{5/P3}$) in Path1 RP3, we expect that pathway Path1 RP3 should be more competitive than Path2 RP3 for the sake of simplicity. Furthermore, pathway Path3 RP3 has the same step of 5 → $TS_{5/6}$ → 6 as pathway Path2 RP3. While in pathway Path3 RP3, 6 transforms to P3 by going through $TS_{6/7}$ (11.50), 7 (−64.20) and $TS_{7/P3}$ (5.36) respectively, a successive methyl-H-shift-elimination reaction steps. Since pathway Path3 RP3 possesses a couple of energy barriers (51.53 and 69.56 kcal/mol see Scheme 1), it is not difficult to draw into conclusion that pathway Path3 RP3

Table 1 Relative energies ($E = U + \mathrm{ZPE}$), enthalpies (H), Gibbs free energies (G) in kcal/mol and entropies (S) in cal $\mathrm{mol}^{-1}\mathrm{K}^{-1}$ of intermediate isomers, transition states and products for the F + propyne reaction

System	E	H	S	G
C1	−0.36	−0.23	−10.88	3.01
C2	−0.32	−0.31	−16.52	4.61
A1	−7.77	−8.31	−24.51	−1.00
1	−40.88	−41.98	−29.46	−33.20
2	−40.73	−41.85	−29.58	−33.03
3	−50.94	−52.03	−29.79	−43.15
4	−40.21	−41.22	−28.52	−32.71
5	−40.28	−41.19	−27.54	−32.98
6	−40.03	−40.93	−28.30	−32.50
7	−64.20	−65.37	−29.87	−56.46
8	−38.26	−39.29	−28.68	−30.74
9	−13.68	−14.6	−27.67	−6.35
$TS_{C1/P1}$	−2.96	−4.44	−23.06	2.43
$TS^{a}_{C1/P1}$	0.28	−1.18	−28.84	7.42
$TS_{C2/P2}$	13.99	13.3	−24.32	20.55
$TS_{A1/1}$	−7.84	−8.75	−27.30	−0.61
$TS^{a}_{A1/1}$	−7.37	−8.12	−26.03	−0.36
$TS_{A1/5}$	−7.78	−8.56	−25.28	−1.02
$TS^{a}_{A1/5}$	−7.61	−8.29	−24.81	−0.89
$TS_{1/2}$	−37.78	−38.6	−29.77	−29.72
$TS_{1/3}$	−0.11	−1.67	−31.46	7.70
$TS_{2/P4}$	12.21	11.37	−26.31	19.21
$TS_{3/4}$	−10.67	−11.98	−30.42	−2.91
$TS_{4/P3}$	5.51	4.23	−29.33	12.97
$TS_{5/P3}$	3.88	2.67	−28.74	11.24
$TS_{5/6}$	−36.57	−37.68	−27.41	−29.51
$TS_{5/8}$	8.25	7.47	−25.44	15.05
$TS_{6/P3}$	3.62	2.44	−28.74	11.01
$TS_{6/P5}$	14.11	13.2	−26.46	21.09
$TS_{6/7}$	11.50	10.68	−30.19	19.68
$TS_{7/P3}$	5.36	4.11	−29.35	12.86
$TS_{8/P4}$	13.25	12.55	−23.97	19.70
$TS_{8/9}$	−13.80	−15.03	−29.66	−6.19
$TS_{9/P5}$	15.45	14.42	−27.81	22.71
P1	−37.90	−37.53	3.44	−38.55
P2	2.78	3.05	4.53	1.70
P3	−4.31	−4.4	−4.19	−3.16
P4	0.52	1.00	−9.76	3.91
P5	8.62	8.82	−3.49	9.86

CCSD(T)/aug-cc-pVDZ//UMP2/6-311++G(d,p) single-point electronic energies and UMP2/6-311++G(d,p) frequencies were used (1 atm and 298.15 K are assumed)

[a] Calculated at Max{CCSD(T)/aug-cc-pVDZ} IRC{UMP2/6-311++G(d,p)} + ZPE level of theory (IRCMax method)

is less competitive than Path1/2 RP3 and can be ruled out from the doublet PES in low-temperature range.

It is obvious that the starting reaction steps R → A1 → $TS_{A1/1}$ → 1 in pathway Path4 RP3 are similar to R → A1 → $TS_{A1/5}$ → 5 in pathway Path1 RP3. Thus, pathway Path4 RP3 may also have negative temperature dependence in low-temperature ranges. In pathway Path4 RP3, a successive four-center-H-shift, three-center-F-migration and fluoromethyl-H-elimination steps 1 → $TS_{1/3}$ → 3 → $TS_{3/4}$ → 4 → $TS_{4/P3}$ → P3 can lead to product P3. It is a typical addition–isomerization–elimination reaction mechanism. Since the rate-determining energy barrier ($TS_{4/P3}$, 5.51) of Path4 RP3 is higher than that of Path1 RP3 ($TS_{5/P3}$, 3.88) and Path2 RP3 ($TS_{6/P3}$, 3.62), pathway Path4 RP3 should be less competitive than Path1/2 RP3.

II. The HCCF (fluoroethyne) + CH_3 formation channel

There are two pathways through which the adduct A1 can transform to the product P4. In pathway Path5 RP4, the characteristic steps are 1 → $TS_{1/2}$ → 2 → $TS_{2/P4}$ → P4 among the whole doublet potential energy surface, a successive alkynyl-H-swing and methyl-elimination

process. While in pathway Path6 RP4, the whole pathway is an F-addition-H-shift-methyl-elimination reaction process. The most noteworthy difference between the two pathways is the site where the methyl is eliminated. As shown in Fig. 1, the transition state $TS_{2/P4}$ shows the rupture of C–C bond between the methyl-C and the fluoroethynyl-C fluorine abutting on, whereas the transition state $TS_{2/P4}$ indicates that methyl eliminates from the fluoroethynyl–C hydrogen abutting on. We should mention that this methyl-elimination process is the only C–C rupture microchannel existing on the ground state potential energy surface. Considering there are two high energy barriers ($\Delta \boldsymbol{G} = 48.03$ kcal/mol for $TS_{5/8}$ and $\Delta \boldsymbol{G} = 50.44$ kcal/mol for $TS_{8/P4}$) in pathway Path6 RP4 whereas there is only one high energy barrier ($\Delta \boldsymbol{G} = 52.24$ kcal/mol for $TS_{2/P4}$) in pathway Path5 RP4 and the rate-determining energy barrier of pathway Path6 RP4 (13.25) is higher than that of pathway Path5 RP4 (12.21), we can safely draw the conclusion that pathway Pa h6 RP4 is less competitive than pathway Path5 RP4.

III. The CH_3CCF (fluoropropyne) + H channel

Clearly, CH_3CCF and CH_2CCHF are isomeric compounds, and the fluoropropyne formation channels include two microchannels, which is pathway Path7/8 RP5. As shown in Fig. 2, the pathways Path2/3 RP3 and Path7 RP5 possess the same reaction steps of R → A1 → $TS_{A1/5}$ → 5 → $TS_{5/6}$ → 6, whereas Path8 RP5 and Path6 RP4 share R → A1 → $TS_{A1/5}$ → 5 → $TS_{5/8}$ → 8 with each other. The difference of the former couple pathways is how intermediate isomer 6 dissociates to relevant products P3 and P5 respectively, whereas for the latter, it is how intermediate isomer 8 dissociates to relevant products P3 and P5 respectively. As the analysis of pathways Path1/2/3 RP3 has been made detailedly in Sect. (I), we therefore discuss the pathway Path7/8 RP5 herein. In pathway Path7 RP5, intermediate isomer 6 can transforms to the product P5 via surmounting $TS_{6/P5}$ (14.11), a 54.51 kcal/mol energy barrier. The latter part of pathway Path7 RP5 is a fluoromethylene-H-elimination reaction mechanism. The high-lying rate-determining transition state $TS_{6/P5}$ may lead us to the fact that pathway Path7 RP5 is less competitive than pathway Path3 RP3 in low-temperature ranges. In pathway Path8 RP5, intermediate isomer 8 (−38.26) can reach the products P5 by going through $TS_{8/9}$ (−13.80), intermediate isomer 9 (−13.68) and $TS_{9/P5}$ (15.45), respectively. Since the transition state $TS_{9/P5}$ is the highest stationary point on the doublet potential energy surface, pathway Path8 RP5 may have the least competitive ability in the reaction at lower temperature, and even at higher temperatures. We should mention that we also tried to locate the H-elimination transition state directly from the fluoromethylene of 5 and the middle carbon of 8, yet all of our attempts failed.

In brief, pathways Path1/2 RP3, Path5 RP4 and Path7 RP5 are the major pathways leading to the three products respectively. Pathway Path1 RP3 is the most competitive pathway while pathway Path7 RP5 is least competitive among the three pathways in low-temperature ranges.

3.1.2 Direct hydrogen abstraction reaction mechanism

For normal propyne $CH_3C{\equiv}CH$, there are two different chemical environments of H-atoms, namely the H in the CH_3 group or the H in the $C{\equiv}CH$ group. The atomic radical F picking up modes would look like below:

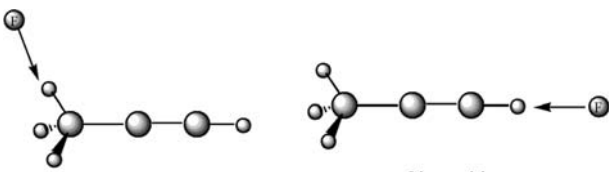

Channel a corresponds to the abstraction of the three equivalent propargyl hydrogens whereas channel b represents the abstraction of the propinyl hydrogen. For convenient discussion, we list them as follows:

Path9 RP1 R → C1 → $TS_{C1/P1}$ → P1 (Channel a)
Path10 RP2 R → C2 → $TS_{C2/P2}$ → P2 (Channel b)

As shown in Figs. 1 and 2, one can find that a loosely bonded intermediate complex (C2) located in the entrance of the hydrogen abstraction process lies −0.32 kcal/mol lower than the reactants, and the corresponding H-abstraction transition state $TS_{C2/P2}$ lies about 14.31 kcal/mol higher than C2. The atomic radical F picking up the H in the $C{\equiv}CH$ group is therefore a two-step abstraction process at 0 K. On the other hand, although the other loosely bonded intermediate complex (C1) prior to the formation of the H-abstraction transition state $TS_{C1/P1}$ along the reaction coordinate was located in the first step of this mechanism involved in the atomic radical F attacking the H-atom in the CH_3 group of propyne, the relative energies of complex C1 lies 0.82 kcal/mol higher than $TS_{C1/P1}$ at Max{CCSD(T)/aug-cc-pVDZ}//IRC{MP2/6-311++G(d, p)} level of theory. This implies that such a complex might be short-lived and not important on the doublet

PES [18,46], and can be safely ruled out from the PES. Therefore the atomic radical F picking up the H atom in the CH_3 group should be a direct hydrogen abstraction mechanism under low temperature conditions [7].

As shown in Fig. 1, corresponding to the direct hydrogen abstraction from CH_3 group of $CH_3C{\equiv}CH$ in pathway Path9 RP1, the geometry of transition state $TS_{C1/P1}$ calculated at the UMP2/6-311++G(d,p) level of theory is found to have a bent structure ($\angle_{F-H-C} = 173.07°$) and an elongated H–F bond length ($r_{F-H} = 1.426$ Å; $r_{C-H} = 1.135$ Å). Most importantly, this geometry is indicative of an "early" transition state, corresponding to a H–F distance significantly longer than the equilibrium bond length (0.917 Å), specifically falling between the HF classical outer turning points of $v = 4$(1.318 Å) and $v = 5$(1.381 Å) [47]. As shown in Fig. 2, it is a barrierlessly exothermic step with the reaction energy of −7.90 kcal/mol at the CCSD(T)/aug-cc-pVDZ//UMP2/6-11++G(d,p) + ZPE level of theory. Since the energies of the transition state and products in this pathway are lower than that of the reactants, the rate of this pathway should be very fast at low-temperature ranges.

Pathway Path10 RP2 corresponds to the possible abstraction of the H atom in C≡CH group of propyne. As shown in Fig. 1, the geometries of transition state $TS_{C2/P2}$ calculated at the three theory level differ much from each other. The angle of $\angle_{F-H-C}$ is 121.73 °, 118.37 ° and 162.92 ° respectively, while the rupture bond length of C1–H is 1.462, 1.444 and 1.293 Å respectively correspond to the UMP2/6-311++G(d,p), UMP2/6-311G(d,p) and UMP2/6-311G levels of theory, respectively. However, one can find that the geometrical parameters of the structures in this system are in good agreement with the UMP2/6-311++G(d,p) and UMP2/6-311G(d,p) levels of theory, while the prediction of geometries at the UMP2/6-311G level departures from that at higher levels to a certain extent. This indicates that for systems similar to the title reaction, the MP2/6-311++G(d,p) level of theory is sufficient to obtain reliable geometrical parameters [16]. As shown in Table 1, the relative energies of transition states and product in pathway Path10 RP2 are higher than those in pathway Path9 RP1. Therefore, both kinetic and thermodynamic considerations may rule out the significance of pathway Path10 RP2. Thus, for the hydrogen abstraction reactions in the title reaction, the HF formation occurs via direct abstraction mechanism dominantly and the H atom picked up by the atomic radical F in the reaction with normal propyne seems to come mostly from the CH_3 group [7].

Before ending this section, we would like to make a short comment on the expected behavior of the pathways at various experimental conditions on the title reaction. At 0 K, in terms of the doublet PES, one can find that both complex C1 (−0.36) and transition state $TS_{C1/P1}$ (−1.18) lie lower than the reactant at Max{CCSD(T)/aug-cc-pVDZ}//IRC{UMP2/6-311 + + G (d,p)} + ZPE level. Considering that the rate-determining transition state $TS_{5/P3}$ lie 3.88 kcal/mol above the reactants in the major pathway Path1 RP3 of the addition–isomerization–elimination reaction mechanism, we can safely make the conclusion that the reaction pathway Path9 RP1 is the most feasible reaction pathway on the doublet potential energy surface in low-temperature ranges. However, under standard conditions (298.15 K and 1 atm.), the formation of C1 is an endergonic process ($\Delta \boldsymbol{G} = 3.01$ kcal/mol, see Table 1). This indicates that C1 may not exist on the PES and the hydrogen abstraction should be a direct process. Further, such process involves considerable barrier ($TS_{C1/P1}\Delta \boldsymbol{G} = 7.42$ kcal/mol). At reaction entrance, the endergonic step may prevent the feasibility of the hydrogen abstraction reaction mechanism. Consequently, it is unlikely that the direct abstraction reaction proceeds facilely under standard conditions. While for the addition channels, the activated complexes A1* can be stabilized efficiently by three body collisions. Therefore, the major reaction pathways should be the association channels forming the C_3H_4F radical. We have shown that the energy barrier associated with '**TS**add' is much lower than that of '**TS**abs' and consequently the C_3H_4F radical should be the most favored product. We expect that once the reaction occurs by three body collisions under high-pressure conditions, the heat released in overall reaction may make the C_3H_4F radical easier to go through the subsequent reaction steps although such process involves moderate barriers ($TS_{5/P3}\Delta \boldsymbol{G} = 11.24$ kcal/mol, etc.). Therefore, the kinetic considerations support the viability of this channel.

3.2 Comparison with experiments

Recently, Ran et al. [7] carried out the kinetic study for the title reaction. In their experiment, two reaction channels have been clearly observed: H + C_3H_3F and HF + C_3H_3. They suggested that the substitution of F for H occurs mainly via a complex formation mechanism, and the HF formation occurs via a direct abstraction mechanism dominantly. Concerning the site specific effects, they proposed that the H atom picked up by the F atom in the reaction with normal propyne seems to come mostly from the CH_3 group, and the H atom produced in the H atom formation channel appears to be mostly from the CH_3 group with some contribution from the CCH group. Our theoretical results are very well consistent with the experimental results mentioned above. In terms of branching ratios determination they pointed out that

the H formation channel is the major reaction pathway, while the HF formation channel is also significant. This significantly differs from our theoretical results. According to our results, the hydrogen abstraction reaction has a lower energy barrier than the hydrogen elimination reaction, and therefore HF + C_3H_3 should be the most favored product. To rationalize this difference, we turn to the experimental conditions. In the crossed molecular beam experiment [7], the energy in the facile formed reactive intermediates are not randomized, coupled with the lifetime of the long-lived complex C_3H_4F radical was long enough for the energy to flow from the activated carbon–carbon σ bond to the breaking carbon–hydrogen bond of the methyl group [48–50]. On the other hand, the collision energy was sufficient (5.2 kcal/mol). The carbon–hydrogen bond rupture of the methyl group forms educts H atom and fluoroallene, therefore it occurs readily. For the HF formation channel, however, it takes place through a direct pickup type mechanism [7] in which the intramolecular vibrational energy redistribution (IVR) may be not necessarily complete and could therefore lead to only a small fraction of collision energy, E_{col}, is converted to the vibrational energy of the intermediates and the dominant fraction goes to their rotational excitation. Herein, a comparison of the present theoretical result with future experimental data will actually address this issue.

In our calculations, one can also find that the rational explanation of the experimental phenomena that H atom elimination from the CCH group occurs at all despite the strong C–H bond. As shown in Fig. 1, from the structures of the H elimination transition states $TS_{6/P5}$ and $TS_{9/P5}$, one can find that the H atoms eliminate from the fluoromethylene ($TS_{6/P5}$) and the middle-C ($TS_{9/P5}$) indeed. The two C-atoms in $TS_{6/P5}$ and $TS_{9/P5}$ hydrogens connected are not triple bond C-atoms actually, since the corresponding C–C bond lengths are 1.286 and 1.295 Å, while they are 1.199 and 1.203 Å at UMP2/6-311++G(d,p) level of theory, respectively.

Furthermore, it should be pointed out that in the title reaction all intermediate isomers and transition states and products involved in the reaction pathway Path5 RP4, $CH_3 + HC{\equiv}CF$ formation channel, which was not observed in the experiment [7], lie below the corresponding stationary points in Path7 RP5. Therefore, it is safe to draw to a conclusion that pathway Path5 RP4 is kinetically favorable than the pathways leading to P5 and further theoretical and experimental studies are still desirable.

Finally, since the reaction entrance is zero-barrier for all the addition–isomerization–elimination channels, once the addition reaction proceeds, the reaction system immediately enter a deep potential well. As shown in Fig. 2, the exit barriers are moderate high for all the addition–isomerization–elimination channels. Undoubtedly, these features will make the formation of long-lived reaction complexes stand a good chance. This is qualitatively consistent with the experimental results [7].

3.3 Comparison with the F + propene reaction

To give a deeper understanding of the reaction mechanism of F + propyne, it is worthwhile to compare the title reaction with that of the analogous reaction F + propene, which has been studied both experimentally [6] and theoretically [18]. Theoretical calculations show that there exist both similarity and discrepancy. In general, the potential energy surface features of the two analogous reactions F + propene/propyne are very similar. Both reactions involve the same initial association way, i.e, the F atoms and unsaturated hydrocarbons approach each other, forming the initial weakly-bound complex before F atoms addition to the C = C/C≡C double/triple bonds with no barrier. Furthermore, which type of the different chemical environments of H-atom is picked up dominantly by the F atoms are the same in the abstraction processes. Theoretically, the H atoms in the CH_3 group abstraction by F atoms are exergonic processes and involves negative barriers in low-temperature ranges. Therefore, both kinetic and thermodynamic considerations support the viabilities of this type of H-atoms picked up. Such a conclusion is in good agreement with experimental observations [6,7]. The discrepancy lies in the barriers in the abstraction and isomerization reaction processes. From the NBO [51–54] analysis, the σ bond between terminal unsaturated C and H atom in propyne and propene can be described as $\sigma_{C-H(propyne)} = 0.781(sp^{1.10})_C + 0.625(s)_H$ and $\sigma_{C-H(propene)} = 0.769(sp^{2.35})_C + 0.640(s)_H$, respectively. The bigger component of the s orbital in the hybridized orbital of C atom to form the C–H bond of propyne leads to a stronger interaction between the C and the H atom, compared with propene. Evidence can also be seen form the C–H bond length of propyne (1.065 Å), which is shorter than that of propene (1.085 Å). As we all know, if the strength of combination between the adjacent atoms is increased, the bond-scission become difficult. Consequently, it is rational that the barrier of the alkynyl hydrogen abstraction ($\Delta \boldsymbol{G} = 20.55$ kcal/mol) is about 9 kcal/mol higher than that of vinyl hydrogen abstraction ($\Delta \boldsymbol{G} \approx 11$ kcal/mol) [18]. On the other hand, the lower reactivity of the C≡C triple bond also leads to the discrepancy in the isomerization barriers between the two reactions. For the F + propene reaction, all intermediates and transition states involved in

the feasible addition–isomerization–elimination channels lie below the reactants. In addition, the exit barriers are moderate high for all the addition–isomerization–elimination channels [18]. However, for the F + propyne reaction, all exit barriers involved lie above the reactants in the addition–isomerization–elimination channels. Anyway, according to the discussions above, one can found that the reaction mechanisms of F + propyne and F + propene are very similar.

4 Conclusions

A detailed theoretical survey on the complex doublet PES of the reaction of atomic radical F with propyne $CH_3C{\equiv}CH$ has been performed at the UMP2 and CCSD(T) levels of theory. Two different mechanisms, the hydrogen abstraction and addition–isomerization–elimination reaction mechanism, are revealed in the present study. For the hydrogen abstraction reactions, i.e., the most probable evolution pathway in the title reaction, the HF formation occurs via direct abstraction mechanism dominantly and the H atom picked up by the atomic radical F should come mostly from the methyl group of normal propyne. On the other hand, for the addition–isomerization–elimination mechanism, the most feasible reaction pathway is the atomic radical F attacking on the C≡C triple bond of propyne with no barrier leading to the weakly-bound adduct A1 followed by the addition of F to the terminal C to form the low-lying intermediate isomer 5. Subsequently, isomer 5 directly dissociates to P3 H_2CCCHF + H. The P4 HCCF + CH_3 formation channel Path4 RP4 is more feasible than the P5 H_3CCCF + H formation channel Path6 RP5, although the feasibility of CH_3 formation channel was excluded in the experiment. Based on the analysis of the energetics of all channels through which the additions and abstraction reactions proceed, we expect that the major reaction channel may vary with experimental conditions for the title reaction. Therefore, future experimental studies on the title reaction are highly desirable under various pressures and temperatures. The present work will provide useful information for understanding the processes of atomic radical F reaction with other unsaturated hydrocarbons.

Acknowledgment This work is supported by the National Natural Science Foundation of China (Nos. 20073014 and 20103003), Excellent Young Teacher Foundation of the Ministry of Education of China, Excellent Young Foundation of Jilin Province and Technology Development Project of Jilin Province (No. 20050906-6). The authors are also thankful for the reviewers' invaluable comments.

References

1. Parson JM, Lee YT (1972) J Chem Phys 56:4658
2. Parson JM, Shobatake K, Lee YT, Rice SA (1973) J Chem Phys 59:1402
3. Shobatake K, Parson JM, Lee YT, Rice SA (1973) J Chem Phys 59:1416
4. Shobatake K, Lee YT, Rice SA (1973) J Chem Phys 59:1435
5. Farrar JM, Lee YT (1976) J Chem Phys 65:1414
6. Ran Q, Yang CH, Lee YT, Shen G, Yang X (2004) J Chem Phys 121:6302
7. Ran Q, Yang CH, Lee YT, Shen G, Wang L, Yang X (2005) J Chem Phys 122:044307
8. Benson SW (1968) Thermaldynamical kinetics. Wiley, NewYork
9. Moehlmann JG, Gleaves JT, Hudgens JW, McDonald JD (1974) J Chem Phys 60:4790
10. Zvijac DJ, Mukamel S, Ross J (1977) J Chem Phys 67:2007
11. Hase WL, Bhalla KC (1981) J Chem Phys 75:2807
12. Clark DT, Scanlan IW (1978) Chem Phys Lett 55:102
13. Kato S, Morokuma K (1980) J Chem Phys 72:206
14. Schlegel HB (1982) J Phys Chem 86:4878
15. Schlegel HB, Bhalla KC, Hase WL (1982) J Phys Chem 86:4883
16. Zhang MB, Yang ZZ (2005) J Phys Chem A 109:4816
17. Robinson GN, Continetti RE, Lee YT (1990) J Chem Phys 92:275
18. Li JL, Geng CY, Huang XR, Sun CC (2006) J Chem Theor Comput (in press)
19. Nesbitt FL, Monks PS, Scanlon M, Stief LJ (1994) J Phys Chem 98:4307
20. Harper WW, Nizkorodov SA, Nesbitt DJ (2000) J Chem Phys 113:3670
21. Harper WW, Nizkorodov SA, Nesbitt D (2001) J Chem Phys Lett 335:381
22. Shiu W, Lin JJ, Liu K (2004) Phys Rev Lett 92:103201
23. Lin JJ, Zhou J, Shiu W, Liu K (2003) Science 300:966
24. Sekusak S, Liedl KR, Sabljic A (1998) J Phys Chem 102:1583
25. Braña P, Menéndez B, Fernández T, Sordo JA (2000) J Phys Chem A 104:10842
26. Frisch MJ, Trucks GW, Schlegel HB et al (1998) Gaussian 98, revision A.11; Gaussian, Inc.: Pittsburgh, PA, 1998
27. Schlegel HB (1986) J Chem Phys 84:15
28. Sponer J, Hobza PJ (2000) J Phys Chem A 104:4592
29. Nguyen MT, Creve S, Vanquickenborne LG (1996) J Phys Chem 100:18422
30. Gonzalez C, Schlegel HB (1990) J Phys Chem 94:5523
31. Purvis GD, Bartlett RJ (1982) J Chem Phys 76:1910
32. Kendall RA, Dunning TH Jr (1992) J Chem Phys 96:6796
33. Woon DE, Dunning TH Jr (1993) J Chem Phys 98:1358
34. Ignatyev IS, Xie Y, Allen WD, Schaefer HF (1997) J Chem Phys 107:141
35. Schlegel HB, Sosa C (1988) Chem Phys Lett 145:329
36. McDouall JJW, Schlegel HB (1989) J Chem Phys 90:2363
37. Farnell L, Pople JA, Radom L (1983) J Phys Chem 87:79
38. Schlegel HB (1986) J Chem Phys 84:4530
39. Stanton JF (1994) J Chem Phys 101:371
40. Sosa C, Schlegel HB (1987) J Am Chem Soc 109:4193
41. Malick DK, Petersson GA, Montgomery JA Jr (1998) J Chem Phys 108:5704
42. Duncan JL, McKean DC, Mallinson PD, McCulloch RD (1973) J Mol Spec 46:232
43. Huber KP, Herzberg G (1979) Molecular spectra and molecular structure. IV. constants of diatomic molecules. Van Nostrand Reinhold Co

44. Hellwege KH, Hellwege AM (ed) (1976) Landolt–Bornstein: Group II: atomic and molecular physics, vol 7: structure data of free polyatomic molecules. Springer Berlin Heidelberg New York
45. Herzberg G (1966) Electronic spectra and electronic structure of polyatomic molecules. Van Nostrand, New York
46. Geng CY, Li JL, Huang XR, Sun CC (2006) Chem Phys 324:474
47. Coxon JA, Hajigeorgiou PG (1990) J Mol Spectrosc 142:254
48. Balucani N, Asvany O, Kaiser RI, Osamura Y (2002) J Phys Chem A 106:4301
49. Mebel AM, Kislov VV, Kaiser RI (2006) J Phys Chem A 110:2421
50. Perri MJ, Van Wyngarden AL, Lin JJ, Lee YT, Boering KA (2004) J Phys Chem A 108:7995
51. Glendening ED, Badenhoop JK, Reed AE, Carpenter JE, Bohmann JA, Morales CM, Weinhold F (2001) (NBO 5.0) Theoretical Chemistry Institute, University of Wisconsin, Madison, WI. http://www.chem.wisc.edu/~nbo5
52. Reed AE, Curtiss LA, Weinhold F (1988) Chem Rev 88:899
53. Reed AE, Weinhold F, Curtiss LA, Pochatko DJ (1986) J Chem Phys 84:5687
54. Carpenter JE, Weinhold F (1988) J Am Chem Soc 110:368